Dalton Transactions

PAPER

Enhanced photoluminescence in $CaMoO_4:Eu^{3+}$ by Gd^{3+} co-doping†

Cite this: *Dalton Trans.*, 2014, **43**, 4779

B. P. Singh,[a] A. K. Parchur,*[b] R. S. Ningthoujam,[c] A. A. Ansari,[d] P. Singh[a] and S. B. Rai[b]

We have studied the luminescence property of $CaMoO_4:Eu^{3+}$. The emission peaks at 590 ($^5D_0 \rightarrow {}^7F_1$) and 613 nm ($^5D_0 \rightarrow {}^7F_2$) for Eu^{3+} are observed after excitation at 266 nm (*i.e.* Mo–O charge transfer band). The peak intensity of the latter dominates over the former indicating an asymmetric environment of Eu^{3+} in EuO_8 polyhedron or parity mixing. Luminescence intensity increases significantly with co-doping of Gd^{3+}. This is ascribed to energy transfer from Mo–O/Gd^{3+} to Eu^{3+}. Luminescence intensity increases with annealing up to 900 °C due to the extent of decrease of non-radiative rates. Very high asymmetric values (A_{21}) of 12–16 are found indicating a red emitter. As-prepared samples are dispersible in polar solvents like water, ethanol, methanol, dimethyl sulfoxide (DMSO) and ethylene glycol (EG); and among them, optimum luminescence is found in methanol. Polymer film shows red emission. The quantum yields of as-prepared 2 and 10 at% Gd^{3+} co-doped $CaMoO_4:Eu^{3+}$ under 277 nm (UV excitation) are 21 and 80%, respectively.

Received 6th October 2013,
Accepted 5th December 2013

DOI: 10.1039/c3dt53408a

www.rsc.org/dalton

1. Introduction

Lanthanide (Ln^{3+}) doped molybdates and tungstates having Scheelite type (ABO_4, A = Ca, Sr, Mg and Ba; B = Mo and W) have been extensively studied by the scientific community as multifunctional materials because of its diverse and prominent applications in acousto-optic filters, solid state lasers, white light emitting diodes (w-LED), scintillations, fluorescent lamps, solar cell, electrolyte material for solid oxide fuel cells and catalysis.[1–3] $CaMoO_4$ reflects its intriguing features having high melting points (1445–1480 °C), refractive index (1.98), photoelectron yield (9%), non-hygroscopic and higher thermal, chemical and mechanical stabilities.[4] It can give a blue to green light under UV excitation depending on particle size. In recent years, calcium molybdate has been extensively studied as a potential phosphor because of higher chemical stability as compared to other fluoride ($NaYF_4$ and/or $BaYF_5$) and oxide materials. Many reports have been published on the photoluminescence of calcium molybdate ($CaMoO_4$) doped with different lanthanide ions.[5–8] Nowadays, much attention is focused on enhancing the luminescent intensity of phosphors. Besides the energy transfer from sensitizer to activator, like Ce^{3+} to Tb^{3+}, another way to improve the efficiency of phosphors is a quantum cutting process.[9] Rare earth ions such as Sm^{3+}, Eu^{3+}, Tb^{3+}, Er^{3+}, Tm^{3+} and Ho^{3+} have been used as luminescence centers because they have their abundant energy levels for radiative transition, and some are suitable for direct pumping by UV/Vis or NIR laser diode.[10–13] Currently, Gd^{3+} based material can be effectively used as a contrast agent in MRI for medical diagnosis and a marker in bio-labeling/bio-imaging.[14] Recently, Eu^{3+} and Er^{3+}/Yb^{3+} doped $GdVO_4$ have shown potential as luminomagnetics under UV excitation.[15,16] Also rare earth doped $NaGdF_4$ has been proposed as a potential bimodal imaging phosphor.[17,18] However, rigorous low efficiency of these nanomaterials stringently confined their pervading applications. Consequently, it will be of great interest and worthy of pursuit to significantly increase the emission intensity of phosphors in order to deploy their potential applications. At these limited conditions for using rare earth ions as emitters in real devices, a better understanding of the excitation and quenching mechanisms should be investigated in detail to optimize their optical properties.

A single-component white-light phosphor is normally produced by co-doping a sensitizer and an activator into the same host matrix. A few significant investigations have been performed to improve the luminescent properties of $CaMoO_4$ phosphor by co-doping of other metal ions. The energy transfer mechanism from a sensitizer to an activator such as $Eu^{2+}/$

[a]*Department of Physics, Indian Institute of Technology (BHU), Varanasi, 221005, India*
[b]*Department of Physics, Banaras Hindu University, Varanasi, 221005, India. E-mail: kareemskpa@hotmail.com, ak.parchur@usu.edu*
[c]*Chemistry Division Bhabha Atomic Research Centre, Mumbai, 400085, India*
[d]*King Abdullah Institute for Nanotechnology, King Saud University, Riyadh, Saudi Arabia-11451*

†Electronic supplementary information (ESI) available. See DOI: 10.1039/c3dt53408a

Mn^{2+}, Ce^{3+}/Mn^{2+}, and Ce^{3+}/Eu^{2+} couples has been investigated in many inorganic hosts, and an effective resonance-type multi polar interaction has been verified in $NaSr_4(BO_3)_3:Ce^{3+}$, Mn^{2+},[19] $Na\text{-}Ba_4(BO_3)_3:Ce^{3+}$, Mn^{2+},[20] $Sr_3Sc(PO_4)_3:Eu^{2+}$, Mn^{2+},[21] $Sr_3B_2O_6:Ce^{3+}$, Eu^{2+},[22] and so on. Moreover, some single-phase phosphors, such as $Ca_{10}K(PO_4)_7:Eu^{2+}$, Mn^{2+}, $Ca_9Y\text{-}(PO_4)_7:Eu^{2+}$, Mn^{2+},[23] $Ca_9Y(PO_4)_7:Ce^{3+}$, Eu^{2+},[24] and $Ca_9Y(PO_4)_7:Ce^{3+}$, Mn^{2+},[25] are used to improve the emission intensity for *n*-UV LED (light emitting diode) applications. Yan *et al.*[26] have reported the improvement in luminescence intensity of three orders of magnitude of $CaMoO_4:5Eu^{3+}$ on Bi^{3+} co-doping. Also an improvement in photoluminescence intensity has been reported with co-doping of charge compensators such as Li^+, K^+, Na^+ and Bi^{3+} in phosphors or with SiO_2 coating over particle of phosphor. In this direction, non-radiative rates are reduced by either charge compensation, improved crystallinity or the extent of decrease of surface dangling bonds/OH bonds by shell from inner core phosphor.[27–29] However, the energy transfer between Eu^{3+}/Gd^{3+} in nanophosphors, which can be synthesized through the auto-combustion route, has rarely been investigated. Gd^{3+} ion is used as co-dopant with Eu^{3+}, Tb^{3+} and/or Dy^{3+} ions in many hosts in order to improve the luminescence.[30,31] The reason for improvement in the luminescence of Ln^{3+} is not understood to date because the emission peak at 310 nm for Gd^{3+} is not fully matched with the absorption band of Ln^{3+}.[9,32] The energy transfer in the case of up-conversion luminescence is generally different from that of down-conversion. There are the following energy transfer processes in down conversion luminescence:[9,29]

(i) Resonance type in which the emission band for the sensitizer (S) is matched with the absorption band of the activator (A) (*i.e.*, S → A),

(ii) Non-radiative energy transfer from higher excited state of M to A,

(iii) Quantum cutting by a two/more-step energy transfer from M to A,

(iv) Increase of absorption cross-section of M and followed by energy transfer from M to A.

Here M represents the phosphor. Upon excitation at any wavelength, the electrons go to the excited state. However, the excited state is either the excited energy levels of M (from electronic or band transition) or simply no excited energy level of M. Excitation energy is usually more than the minimum absorption energy of A.

In this article, we have prepared Gd^{3+} (0, 2, 5, 7 and 10 at%) co-doped $CaMoO_4$:Eu nanoparticles *via* an efficient auto-combustion technique. For the optimal Eu^{3+} concentration (2 at% in this study), prominently enhanced red emission of Eu^{3+} is obtained for the as-prepared, 600 and 900 °C annealed samples by addition of Gd^{3+} co-doping instead of varying the Eu^{3+} concentration. Their structural property has been reported by B. P. Singh *et al.* elsewhere.[33] The photoluminescence property of Gd^{3+} co-doped $CaMoO_4$:Eu has been investigated in detail for ASP, 600 and 900 °C annealed samples. It may be a potential suitable red phosphor material which is the bottleneck for the advancement in white LED at much lower cost.

2. Experimental details

Gd^{3+} (0, 2, 5, 7 and 10 at%) co-doped $CaMoO_4$:Eu nanoparticles were prepared *via* a facile auto-combustion technique. As-prepared sample (ASP) was annealed at 600 and 900 °C for 4 h each.[33] The concentration of Eu^{3+} is fixed at 2 at%. Samples show tetragonal phase. Crystallinity increases with an increase in annealing temperature. As-prepared sample, 600 and 900 °C annealed samples are considered as ASP, 600 °C and 900 °C, respectively. The UV/Vis absorption spectra were measured on a Perkin-Elmer Lambda-40 spectrophotometer in the range 190–600 nm, with the sample contained in a 1 cm^3 stoppered quartz cell of 1 cm path length. Photoluminescence excitation spectra of the samples were recorded using Hitachi F-4500 spectrometer equipped with a 150 W Xe lamp as a source having spectral resolution of 3 nm. Photoluminescence spectra were studied by a 266 nm pulsed Nd-YAG laser (Spitlight 600, Innolas, Germany) source. Photoluminescence decay was recorded with an Edinburgh instrument F-920 equipped with a 100 W μs flash xenon lamp as the excitation source. All measurements were performed at room temperature.

3. Results and discussion

3.1 Absorption studies

Optical band gap energy for ASP, 600 and 900 °C was calculated using a model proposed by Wood and Tauc.[34] According to this model, the optical band gap follows the relation as:

$$\alpha h\nu \propto (h\nu - E_g)^n \quad (1)$$

where α is the absorbance, h is the Planck constant, ν is the frequency, E_g is the optical band gap of the nanomaterial. The exponent n is a constant which can have values n = 1/2, 2, 3/2 or 3 depending on the form of transition, *i.e.*, direct allowed, indirect allowed, direct forbidden and indirect forbidden transitions, respectively. The literature supports that molybdates have an optical absorption governed by direct electronic transitions.[1,2] A typical energy gap calculation of 5 at% Gd^{3+} co-doped $CaMoO_4$:Eu for ASP, 600 and 900 °C samples from absorption spectra is shown in Fig. 1 and estimated values are found to be ~5.07, 4.71 and 4.68 eV, respectively. The decrease in energy band gap of the host is related to the increase of particle size upon annealing.[2,33,35]

4.2 Photoluminescence study

4.2.1 Excitation study. Fig. 2(a) shows the excitation spectra of ASP sample of Gd^{3+} (0 and 10 at%) co-doped $CaMoO_4$:Eu, monitoring the emission wavelength at 613 nm. The broad peak at 220–350 nm and sharp peaks with low intensity between 350–550 nm are observed. These broad peaks arise due to overlap of Eu–O and Mo–O charge transfers (CT).[36–38] Peaks at 247 and 272 nm are assigned to be Eu–O and Mo–O CT band, respectively.[6] The sharp excitation peaks

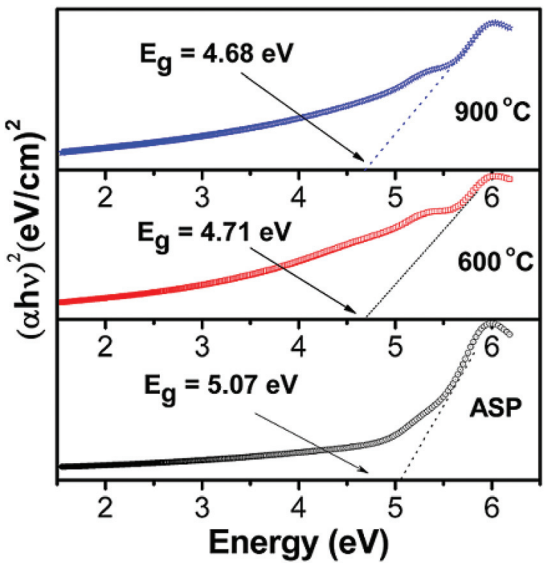

Fig. 1 $(\alpha h\nu)^2$ *vs.* $h\nu$ for ASP, 600 and 900 °C annealed samples of 5 at% Gd^{3+} co-doped $CaMoO_4$:Eu in absorption spectra.

due to intra-configurationally f–f transitions of Gd^{3+} ions were reported at 255 nm ($^8S_{7/2}\rightarrow{}^6D_{9/2}$), 275 nm ($^8S_{7/2}\rightarrow{}^6I_{11/2}$) and 277 nm ($^8S_{7/2}\rightarrow{}^6I_{9/2}$).[9] While peaks at ~362, 376, 382, 396, 412, 466 and 532 nm are assigned to $^7F_0\rightarrow{}^5D_4$, $^7F_0\rightarrow{}^5G_3$, $^7F_0\rightarrow{}^5G_4$, $^7F_0\rightarrow{}^5L_6$, $^7F_0\rightarrow{}^5D_3$, $^7F_0\rightarrow{}^5D_2$ and $^7F_0\rightarrow{}^5D_1$, respectively of intra-configurationally f–f transitions of Eu^{3+} ions. The absorption peaks for Gd^{3+} overlap with Eu–O and Mo–O CTB. On monitoring the emission wavelength of Eu^{3+} at 613 nm, there are strong broad peaks at 220–350 nm and weak peaks at 350–550 nm. This confirms an efficient energy transfer from Gd^{3+}/Mo–O/Eu–O to Eu^{3+}. It is ascribed from the excitation spectra that the intensity of the Gd^{3+}/Mo–O CT absorption band increases for higher concentrations of Gd^{3+} (10 at%) co-doped samples than the Gd^{3+} free samples of ASP, 600 and 900 °C annealed samples. Here, concentrations of Mo^{6+} and Eu^{3+} are fixed in all samples. The increase of intensity in 320–250 nm with increasing Gd^{3+} indicates that there is energy transfer from Gd^{3+} to Eu^{3+} by possible processes (ii–iv) mentioned in the Introduction section. Here process (i) will be at a minimum since there is the least overlapping of the emission band at 313 nm ($^6P_{7/2}\rightarrow{}^8S_{7/2}$) for Gd^{3+} with the absorption band of Eu^{3+}.

Similar reports on the effects of Gd^{3+} have been reported on the Tb^{3+} activated $Ca_2Gd_8Si_6O_{26}$ nanophosphors.[39] It is worthy to mention from Fig. 2(a) that the Gd/Mo–O CT band around 275 nm peak is more symmetrical for Gd^{3+} free $CaMoO_4$:Eu than 10 at% Gd^{3+} co-doped $CaMoO_4$:Eu. More broadening and asymmetricity have been observed for the 10 at% Gd^{3+}

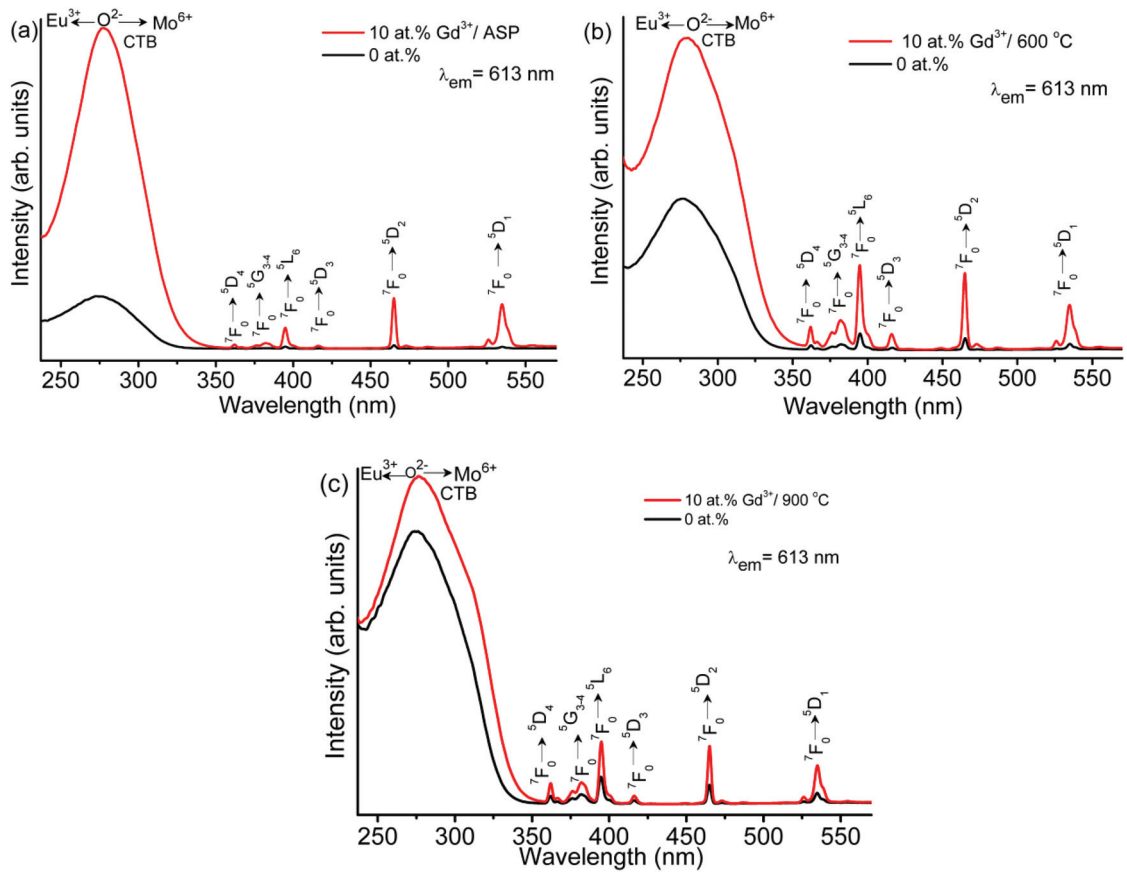

Fig. 2 Excitation spectra of Gd^{3+} (0, 2, 5, 7 and 10 at%) co-doped $CaMoO_4$:Eu nanoparticles: (a) ASP, (b) 600 and (c) 900 °C annealed samples (monitoring emission at 613 nm).

co-doped $CaMoO_4$:Eu samples annealed at 600 and 900 °C than for the Gd^{3+} free sample of $CaMoO_4$:Eu. The variation in intensity of the Gd/Mo–O CT band at around 275 nm was higher than that of the ($^7L_0 \rightarrow {}^5L_6$) transition at ~395 nm; and the intensity of $^7F_0 \rightarrow {}^5D_2$ at 465 nm is higher than that of 395 ($^7L_0 \rightarrow {}^5L_6$) of Eu^{3+} ions (*i.e.*, Gd/Mo–O CT band > 465 nm > 532 nm > 395 nm) for ASP samples. Fig. 2(b) and (c) show the excitation spectra of 600 and 900 °C annealed samples monitoring the emission wavelength at 613 nm. Peaks are similar to that of the ASP samples. For 600 and 900 °C annealed samples, it is observed that in the longer wavelength region, the intensity of the peak ($^7L_0 \rightarrow {}^5L_6$) at 396 nm is higher than that at 465 nm ($^7F_0 \rightarrow {}^5D_2$) and 532 nm ($^7F_0 \rightarrow {}^5D_1$). As the annealing temperature increases, it is observed that the Eu–O/Mo–O CT band maximum is shifted towards the lower energy side. It is related to an increase in covalent character of Eu–O/Mo–O.[40,41]

4.2.2 Emission study. Emission spectra of Gd^{3+} (Gd^{3+} = 0, 2, 5, 7 and 10 at%) co-doped $CaMoO_4$:Eu (ASP, 600 and 900 °C annealed samples) are shown in Fig. 3 under 266 nm Nd-YAG laser excitation. The spectrum shows a strong emission peak at 613 nm. It is observed that incorporation of Gd^{3+} ion in $CaMoO_4$:Eu does not have an effect on the shape of the spectra but does change the PL intensity enormously. Emission spectra comprise five characteristic emission lines of Eu^{3+} which are originated from $^5D_1 \rightarrow {}^7F_1$ and $^5D_0 \rightarrow {}^7F_j$ (j = 1, 2, 3, 4). The emission peaks at ~590 ($^5D_0 \rightarrow {}^7F_1$) and 613 nm ($^5D_0 \rightarrow {}^7F_2$) are assigned to magnetic and electric dipole transitions of Eu^{3+}, respectively. The $^5D_0 \rightarrow {}^7F_2$ transition is hypersensitive and found to be dominant over all peaks in the spectra. It is found that the emission intensity of Eu^{3+} increases with Gd^{3+} up to 2 at% Gd^{3+} for ASP samples and then decreases. This may be due to the surface defects and concentration quenching effect. PL intensity increases up to 7 at% and 10 at% Gd^{3+} for 600 and 900 °C annealed samples, respectively. This may be due to the extent of reduction of nonradiative rates coming from the surface dangling bonds, water molecules adsorbed at the surface and removal of –NO and –CH groups upon annealing at higher temperatures.

In order to compare the emission intensities of electric and magnetic dipole transitions, the Gaussian function is used to

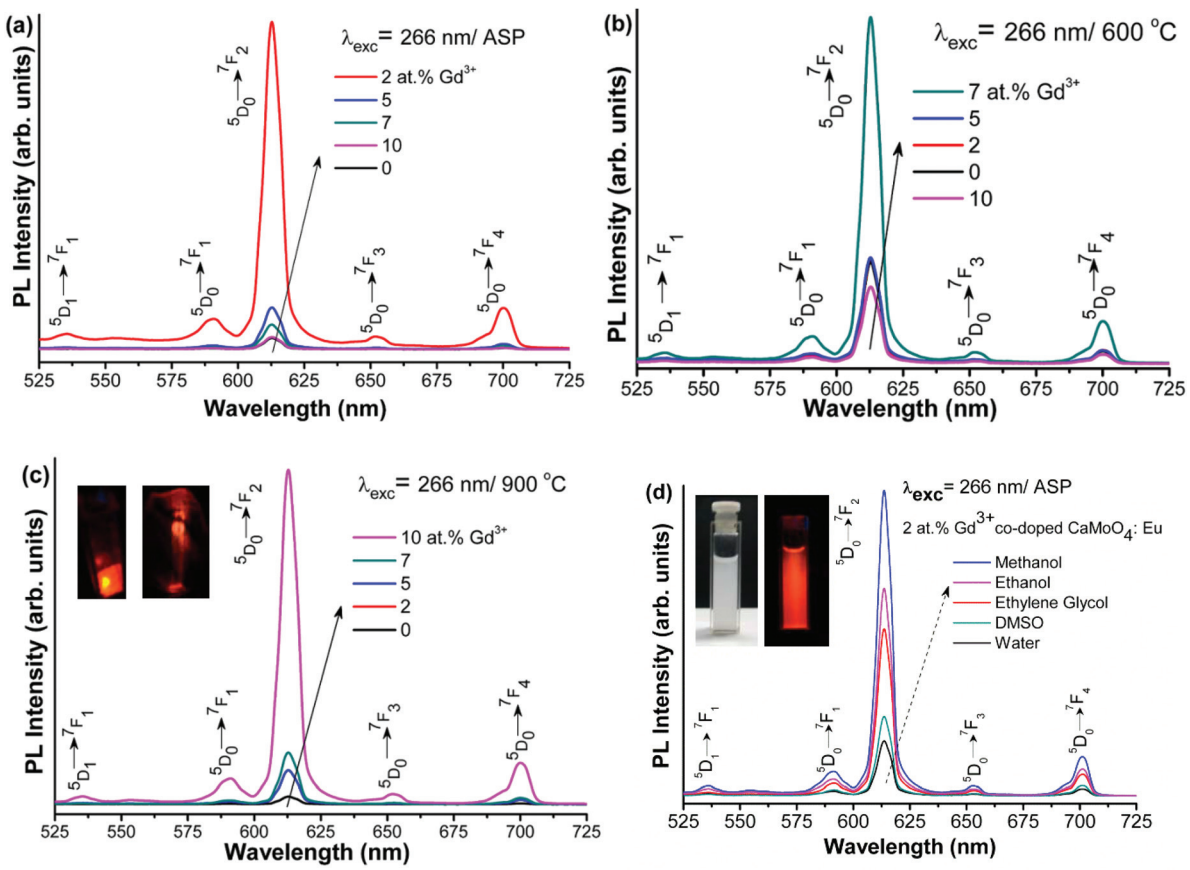

Fig. 3 Luminescence spectra of Gd^{3+}(0, 2, 5, 7 and 10 at%) co-doped $CaMoO_4$:Eu nanoparticles: (a) ASP, (b) 600 (c) 900 °C (inset shows the digital photographs of powdered sample and polymer film under 266 nm laser excitation of 2 at% Gd^{3+} co-doped $CaMoO_4$:Eu) and (d) PL emission spectra in different solvents *viz.* water, ethanol, methanol, DMSO and EG of ASP 2 at% Gd^{3+} co-doped $CaMoO_4$:Eu (inset shows the digital photographs of dispersed solution in EG before and after irradiation under 266 nm Nd-YAG source excitation).

fit the curve. The magnetic and electric dipole transitions are fitted by the relation as;

$$I = I_B + \frac{A_1}{w_1\sqrt{\pi/2}} e^{2[(\lambda-\lambda_{c1})^2/w_1^2]} + \frac{A_2}{w_2\sqrt{\pi/2}} e^{2[(\lambda-\lambda_{c2})^2/w_2^2]} \quad (2)$$

where I is the intensity, I_B is the background intensity, A is the area of the corresponding peaks, w is the FWHM, λ is the wavelength, while λ_c is the average value to the assigned transitions. These peaks are fitted well in the range 580–600 nm for magnetic and 600–630 nm for electric dipole transitions, respectively. Typical fitting data of magnetic to electric dipole transitions of 5 at% Gd^{3+} co-doped $CaMoO_4$:Eu sample annealed at 600 °C under ~266 nm excitation is shown in the Fig. S1(ESI†). It is well fitted with a value of χ^2 = 0.9967. The values of the fitting parameters are marked in the figure itself. The detailed analyses of peak position of magnetic $^5D_0 \rightarrow {}^7F_1$ and electric dipole transition $^5D_0 \rightarrow {}^7F_2$ and FWHM of Gd^{3+} (0, 2, 5, 7 and 10 at%) co-doped $CaMoO_4$:Eu for ASP, 600 and 900 °C heated samples are listed in Table S1 (ESI†). Emission peaks corresponding to magnetic and electric dipoles after Gaussian profile curve fitting to assigned transition do not shift to a great extent but FWHM values of the peaks decrease gradually for ~600 and 900 °C heated samples of Gd^{3+} (0, 2, 5, 7 and 10 at%) co-doped $CaMoO_4$:Eu. Fig. 4(a) shows the variation of intensities (integrated area under curve) for ASP, 600 and 900 °C annealed samples of Gd^{3+} (0, 2, 5, 7 and 10 at%) co-doped $CaMoO_4$:Eu. A slight improvement in the peak profile intensity for 600 °C is observed as compared to the ASP one while peak intensities (integrated area under the curve) are significantly higher for the 900 °C samples. Comparatively low luminescence intensity is observed for 600 °C as compared to 900 °C annealed samples because at lower temperature, the particle having ample surface to volume ratio, leads to a sufficient amount of non radiative transitions. In the case of the 900 °C annealed samples, particles have a lower surface to volume ratio which results in a decrease of nonradiative transitions and hence improved photoluminescence is observed. Similar behaviour has been reported for the Eu^{3+} doped $GdVO_4$ system.[42] The asymmetric environment of the Eu^{3+} ion in the host lattice can be calculated by the integrated intensity ratio of electric ($^5D_0 \rightarrow {}^7F_2$) to magnetic ($^5D_0 \rightarrow {}^7F_1$) dipole transitions. It is termed the asymmetric ratio represented as A_{21}, where subscript '2' and '1' refer to transitions of $^5D_0$ to ^7F_j, j = 2 and 1, respectively. In a site with inversion symmetry, the $^5D_0 \rightarrow {}^7F_1$ transition is dominant while in a site without inversion symmetry, the $^5D_0 \rightarrow {}^7F_2$ transition dominates.[43]

A_{21} is calculated as;

$$A_{21} = \frac{\int_{600}^{630} I_2 d\lambda}{\int_{580}^{600} I_1 d\lambda} \quad (3)$$

where I_2 and I_1 are the intensities of electric and magnetic dipole transitions, respectively calculated after background correction subjected to the peaks under Gaussian fit and λ is the wavelength. Photoluminescence spectra reveal that maximum intensity occurs at 613 nm $^5D_0 \rightarrow {}^7F_2$ hypersensitive electric dipole transition which is highly sensitive to the asymmetric environment around Eu^{3+}. Hence the variation in peak intensity of electric dipole transitions with respect to Gd^{3+} concentration under ~266 nm excitation is studied. The A_{21} value increases upon annealing the sample at 600 and 900 °C as compared to ASP (Fig. 4(b)). A_{21} values for 5 at% Gd^{3+} co-doped $CaMoO_4$:Eu in case of ASP, 600 and 900 °C annealed samples are found to be ~13.49, 14.60 and 15.95, respectively. In the present study, maximal values of A_{21} are found up to ~16 under ~266 nm Nd:YAG laser excitation. This higher value in A_{21} signifies that higher local disorder/distortion occur in the Gd^{3+} co-doped $CaMoO_4$:Eu host lattice and lattice distortion induces more odd-rank crystal field components such as $4f^5 5d$ mixed into the electronic transition levels of $4f^6$ of Eu^{3+} after Gd^{3+} addition and hence enhances the photoluminescence intensity significantly. A similar trend in the A_{21} value has been reported in the literature for Eu^{3+} doped $(Li, Na)_2(Gd_4MoO_4)_7$ under a ~466 nm lamp excitation and for bis-β diketonate lanthanide complexes.[44,45] Parchur *et al.*[5] has reported the asymmetric ratio of Eu^{3+} under different lamp

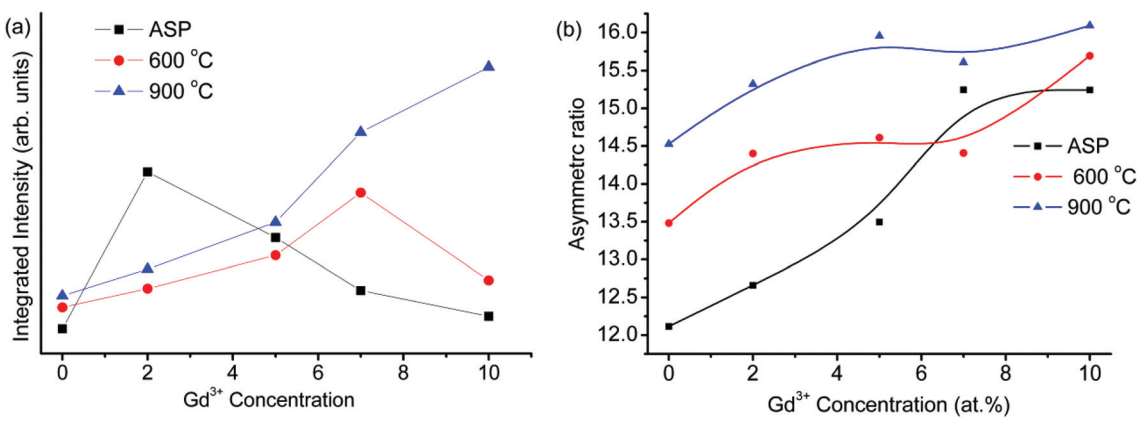

Fig. 4 (a) Photoluminescence intensity variation of Gd^{3+} co-doped (0, 2, 5, 7 and 10 at%) $CaMoO_4$:Eu of ASP, 600 and 900 °C annealed samples and (b) Asymmetric ratio A_{21} variation of Gd^{3+} co-doped (0, 2, 5, 7 and 10 at%) concentration of $CaMoO_4$:Eu of ASP, 600 and 900 °C annealed samples. Excitation is under a 266 nm Nd-YAG laser.

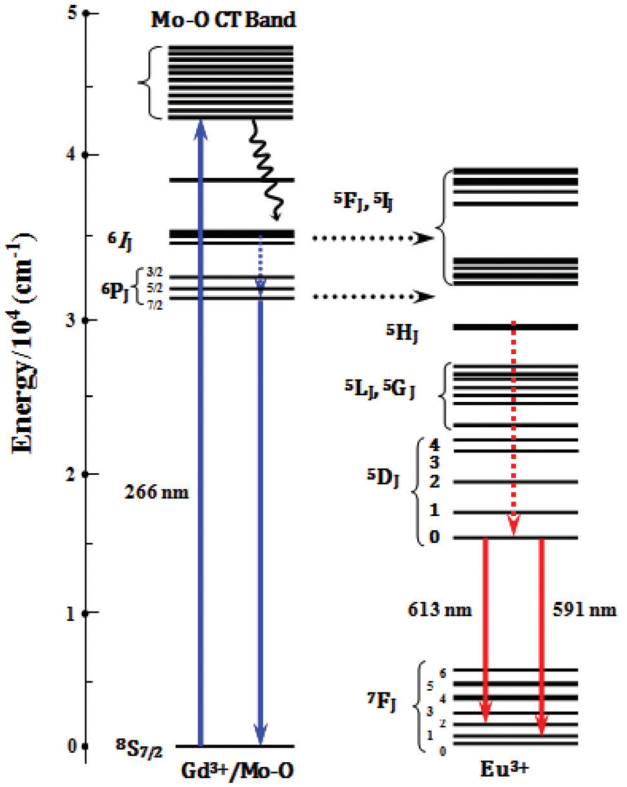

Fig. 5 Schematic energy level diagram for the transfer process between Gd^{3+}/MoO_4^{2-} and Eu^{3+} ions in $CaMoO_4$.

excitation sources and found the value to be in the range of ~2–10 with Eu^{3+} concentration in $CaMoO_4$:Eu. The asymmetric ratio calculated for ASP, 600 and 900 °C under ~266 nm excitation with Gd^{3+} (0, 2, 5, 7 and 10 at%) co-doped $CaMoO_4$:Eu samples is shown in Fig. 4(b).

Fig. 5 shows the schematic diagram of energy levels in Gd^{3+} co-doped $CaMoO_4$:Eu. The band gap of $CaMoO_4$ is ~4.6–5.1 eV (Fig. 1), which is comparable with the Eu–O charge transfer band (4.8–5.1 eV = 240–260 nm) and greater than the Gd^{3+} absorption band at ~3.96 eV. However, there is a weak absorption band at 240–255 nm for Gd^{3+}.[9] Because of the decrease in surface defect or capping ligands on the particle surface, the band gap of the samples slightly decreases on annealing at 600 and 900 °C, which is also supported by UV-Visible absorption measurement (Fig. 1). After excitation at ~266 nm (4.66 eV), the excited electrons go from the Mo–O CT band/Gd^{3+} band (^6I_J) to the excited state of Eu^{3+} ion and relax to ground state levels of Eu^{3+} ion with strong emission at red color regions.

4.2.3 Solvent effect on emission intensity and polymer film studies. ASP sample of 2 at% Gd^{3+} co-doped $CaMoO_4$:Eu proved to be useful for the easy dispersion of nanoparticles in polar solvents like water, ethanol, methanol, dimethyl sulfoxide (DMSO) and ethylene glycol (EG). For a typical dispersion of the nanoparticles, 10 mg of ASP sample of 2 at% Gd^{3+} co-doped $CaMoO_4$:Eu, is dispersed in 10 ml of water, ethanol, methanol, DMSO and EG followed by ultrasonication. Well dispersed nanoparticles in polar medium could be verified up to ~1–2 months without settlement. This may be due to hydrogen bonding between the MoO_4^{2-} unit and/or functional group of the polar solvent. Fig. 3(d) shows the emission spectra of re-dispersed 2 at% Gd^{3+} co-doped $CaMoO_4$:Eu in different solvents *viz.* water, ethanol, methanol, DMSO and EG under 266 nm laser excitation. For all the solvents, f–f transitions of Eu^{3+} were well observed and the intensity of the $^5D_0 \rightarrow {}^7F_2$ transition (red) was found to be more significant. The order of intensity was found to be highest for methanol amongst the other solvents. The polarity index of methanol is minimal amongst the other solvents.[46] High polarity index means a large number of quenching sites and thus, solvents with higher polarity index will have a lower luminescence intensity. It is observed that peak positions of magnetic and electric dipole transitions are unaffected after dispersion of the nanoparticles into these polar solvents. Asymmetric ratio A_{21} obtained for these solvents is not altered significantly as compared to powdered samples. For a typical thin film processing of 2 at% Gd^{3+} co-doped $CaMoO_4$:Eu, 5 mg of ASP sample was mixed with 5 ml of distilled water. After that 0.5 g of PVA and 5 ml of ethanol was added. For uniform dispersion of the sample, it was ultrasonicated for 30 min. This solution was poured into a poly Petri dish. It was kept for 2–3 days at room temperature for drying purposes. In this way polymer films having a thickness of ~0.2–0.3 mm and a diameter of ~10 cm of 2 at% Gd^{3+} co-doped $CaMoO_4$:Eu were prepared. In the inset of Fig. 3(c), it is evident that the film shows bright red under 266 nm laser excitation. Uniform brightness of the thin film confirms the homogeneous distribution of the particles in the polymer matrix. PL spectrum of PVA thin film after incorporation of re-dispersed particles of ASP 2 at% Gd^{3+} co-doped $CaMoO_4$:Eu at 266 nm laser excitation is shown in Fig. S2 (ESI†). It is observed that emission intensities of ASP nanoparticles re-dispersed in water, ethanol, methanol, DMSO, EG and in PVA matrix are slightly less in comparison to powdered samples. This is due to the smaller concentration of Eu^{3+} ion per unit volume of dispersion.

4.2.3 Quantum yield study. Luminescence quantum yield (η) of samples is calculated on the basis of the absolute method. This is related to the ratio of the number of photons absorbed (α) to the number of photons emitted by the sample (ε) as

$$\eta = \frac{\varepsilon}{\alpha} = \frac{\int I_{\text{emission}}}{\int I_{\text{solvent}} - \int I_{\text{sample}}}, \quad (4)$$

where I_{emission} is the luminescence emission spectrum of the sample, I_{solvent} is the spectrum of the light used to excite only the solvent, and I_{sample} is the spectrum of light used for exciting the sample in solvent. Detailed quantum yield experimental set up has been reported in the literature.[47] All spectra are collected using the integrating sphere. Here, solvent was 1 g of PEG dispersed in 100 ml of distilled water. Excitation and emission wavelengths were monitored at 277 nm (absorption peak of Gd^{3+}) and 615 nm. Typical PL spectra of 2 at% Gd^{3+} co-doped $CaMoO_4$:Eu (ASP) for the quantum yield are shown in Fig. 6. The luminescence quantum yields for 2 and

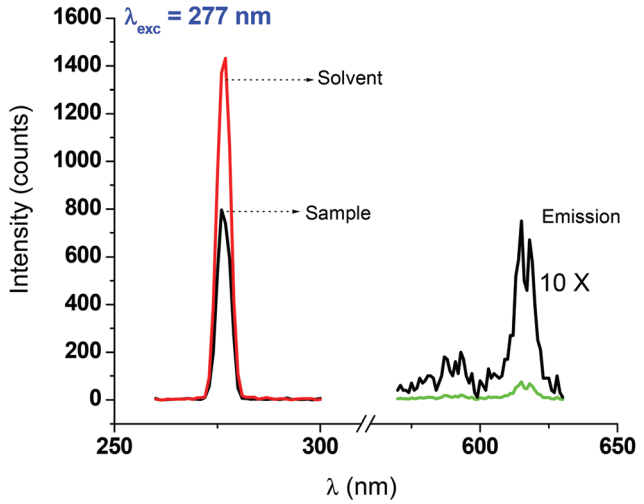

Fig. 6 PL spectra of 2 at% Gd^{3+} co-doped $CaMoO_4$:Eu (ASP) for the quantum yield study.

10 at% Gd^{3+} co-doped $CaMoO_4$:Eu (ASP) are 21 and 80%, respectively. The high quantum efficiency (200%) was reported in Ln^{3+} doped $LiGdF_4$ under VUV excitation.[48]

4.2.4 Photoluminescence decay study. Photoluminescence decay profile of $^5D_0$ (613 nm) level of Eu^{3+} for ASP, 600 and 900 °C annealed samples of Gd^{3+} (0, 5 and 10 at%) co-doped $CaMoO_4$:Eu samples under 277 and 395 nm excitations have been shown in Fig. 7–9. Emission wavelength was fixed at 613 nm. It shows the decay profile of the $^5D_0 \rightarrow {}^7F_2$ transition excited at two different excitations ~277 nm (Gd^{3+}/MoO_4^{2-}) and 395 nm (direct excitation of Eu^{3+}).

Typical plot for 600 °C annealed 5 at% Gd^{3+} co-doped $CaMoO_4$:Eu under 277 nm excitation using mono-exponential [$I = I_0 e^{(-t/\tau)}$, where I_0 and I are the intensities at t = 0 and at time t, respectively and τ is the parameter defining the lifetime of the transition involved in which the intensity drops to (1/e)] decay is shown in Fig. 10(a) and the ln(I) *vs.* t plot is shown in the inset figure for the same. Fitting parameters are given in the figure itself. From the inset of Fig. 10(a), it is evident that the decay curve deviates from the mono-exponential curve fit. Therefore, in the case of 277 nm (Gd/Mo–O) excitation, the luminescence decay curve for $^5D_0 \rightarrow {}^7F_2$ has been fitted using the diffusion equation as

$$I = I_1 \exp(-t/\tau_1 - Dt^{0.5}) - I_2 \exp(-t/\tau_2) + I_b \quad (5)$$

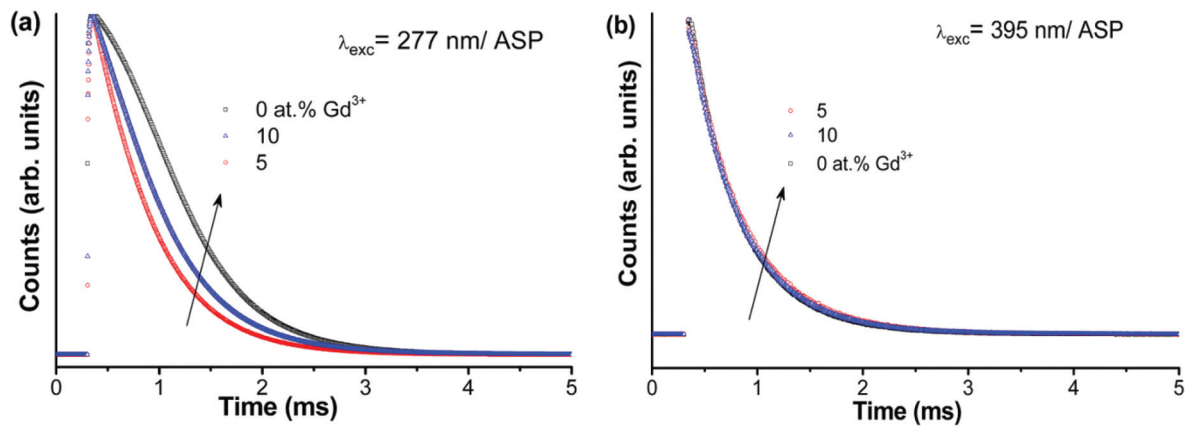

Fig. 7 Luminescence decay spectra of ASP Gd^{3+} (0, 5 and 10 at%) co-doped $CaMoO_4$:Eu nanoparticles at (a) 277 and (b) 395 nm excitations.

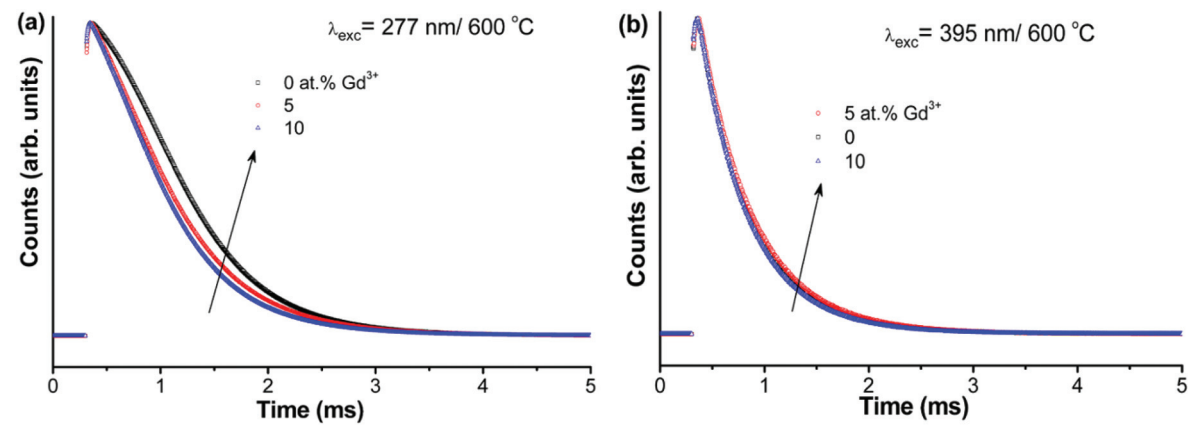

Fig. 8 Luminescence decay spectra of 600 °C Gd^{3+}(0, 5 and 10 at%) co-doped $CaMoO_4$:Eu nanoparticles at (a) 277 and (b) 395 nm excitations.

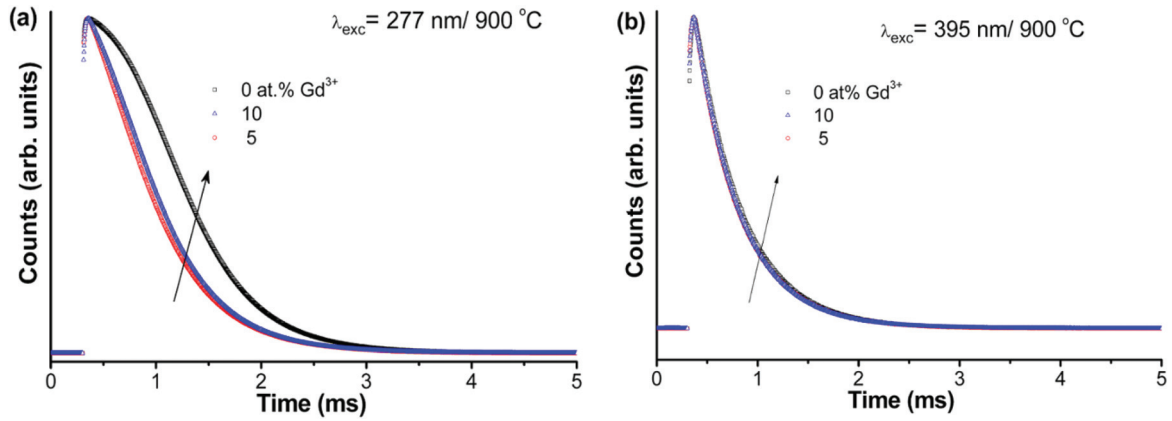

Fig. 9 Luminescence decay spectra of 900 °C Gd^{3+}(0, 5 and 10 at%) co-doped $CaMoO_4$:Eu^{3+} nanoparticles at (a) 277 and (b) 395 nm excitations.

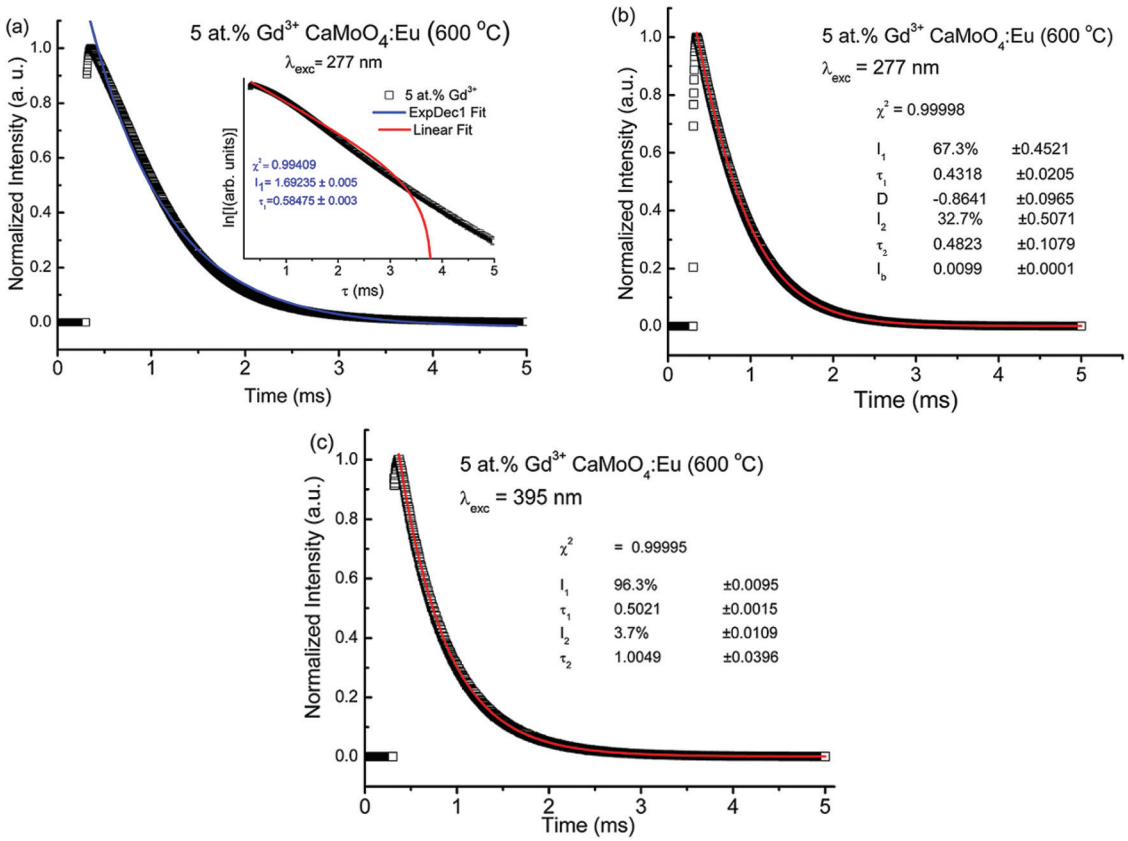

Fig. 10 Fitting of (a) mono-exponential equation and (b) equation associated diffusion and energy transfer (D) to luminescence decay curve (λ_{em} = 613 nm) of 600 °C annealed 5 at% Gd^{3+} co-doped $CaMoO_4$:Eu (λ_{exc} = 277 nm). Fitting parameters are shown in the figure itself. Inset of (a) shows the ln(*I*) *vs.* *t* plot. (c) bi-exponential fitting to the decay curve (λ_{em} = 613 nm) of 600 °C annealed 5 at% Gd^{3+} co-doped $CaMoO_4$:Eu (λ_{exc} = 395 nm).

where I_1, I_2 and I_b are the intensity parameters while D is the diffusion parameter and energy transfer rate. The χ^2 is the goodness of fit and can be expressed as

$$\chi^2 = \Sigma_k w_k{}^2 [X_k - F_k]^2 / n \quad (6)$$

where w_k is a weighting factor for data points $\left(w_k = \frac{1}{\sqrt{F_k}}\right)$, X_k is the fitted data and F_k is the luminescence decay data. Typical fitting of 5 at% Gd^{3+} co-doped $CaMoO_4$:Eu annealed at 600 °C at 277 nm excitation has been shown in Fig. 10(b). Parameters obtained using eqn (5) are given in the figure itself. Fitting parameters obtained for ASP, 600 and 900 °C annealed Gd^{3+} co-doped $CaMoO_4$:Eu samples are listed in Table 1. There are two components of lifetime. The lifetime (τ_1) associated with Diffusion and energy transfer rate (termed as D) is shorter than another one (τ_2). It means that at the initial stage, the

Table 1 Parameters obtained after fitting of [$I = I_1\exp(-t/\tau_1 - Dt^{0.5}) - I_2\exp(-t/\tau_2) + I_b$] equation to the decay data of as-prepared, 600 and 900 °C samples at 277 nm excitation

Sample	Gd^{3+} (at%)	I_1 (%)	τ_1 (ms)	D ($s^{-0.5}$)	I_2 (%)	τ_2 (ms)	I_b	χ^2
ASP	0	42	0.30	−0.7	58	0.48	0.0018	0.99997
	5	51	0.46	−1.3	49	0.58	0.0032	0.99994
	10	53	0.42	−1.3	47	0.52	0.0017	0.99997
600 °C	0	28	0.22	−2.4	72	0.55	0.0024	0.99998
	5	67	0.43	−0.8	33	0.48	0.001	0.99998
	10	44	0.37	−2.0	56	0.58	0.0021	0.99990
900 °C	0	39	0.27	−1.3	61	0.43	0.0009	0.99991
	5	48	0.38	−1.6	52	0.52	0.0019	0.99995
	10	50	0.42	−1.6	50	0.56	0.0025	0.99993

decay is fast. However, τ_1 and τ_2 have almost equal amounts. The τ_2 in the case of the Gd doped sample is slightly longer than that without Gd. τ_1 = 0.22–0.46 ms and τ_2 = 0.43–0.58 ms.

All decay curves are fitted under 395 nm excitation using bi-exponential curve fitting which is expressed as

$$I = I_1 e^{(-t/\tau_1)} + I_2 e^{(-t/\tau_2)} \quad (7)$$

where I_1 and I_2 are the intensities at different time intervals and τ_1 and τ_2 are their corresponding lifetimes, respectively. The average lifetime τ_{av} is calculated as

$$\tau_{av} = (I_1\tau_1 + I_2\tau_2)/(I_1 + I_2) \quad (8)$$

Bi-exponential fitting behaviour corresponds to inhomogeneous distribution of activator ions (Eu^{3+}) in the $CaMoO_4$ host matrix. The shorter lifetime (τ_1) has a greater contribution than the longer one (τ_2). The amount of longer lifetime (τ_2) decreases upon increasing annealing. Even, 900 °C annealed samples follow mono-exponential decay. The average lifetime (τ_{av}) of the sample doped with Gd has a longer lifetime than that without Gd. The τ_1 = 0.41–0.50 ms and τ_2 = 0.65–1.29 ms are found. Fitting parameters (I_1, τ_1, I_1, τ_2, τ_{av} and χ^2) calculated using the bi-exponential curve fit for ASP, 600 and 900 °C annealed samples of Gd^{3+} co-doped $CaMoO_4$:Eu samples are listed in Table 2. Typical bi-exponential fitting of 5 at% Gd^{3+} co-doped $CaMoO_4$:Eu annealed at 600 °C under 395 nm excitation is shown in Fig. 10(c). The average life time value was reported as ~0.459 ms for 5 at% Eu^{3+} doped $CaMoO_4$ under 398 nm excitation.[5] Typical bi-exponential decay fitting for 10 at% Gd^{3+} co-doped $CaMoO_4$:Eu samples annealed at 900 °C and their weighted residuals is shown in Fig. S4 (ESI†). The residuals decay plot is more informative and in fact it demonstrates where the misfit occurs in the curve. The residual *vs.* independent variable plot is shown at the bottom of Fig. S4 (ESI†).

Table 2 Parameters obtained after bi-exponential fit to the decay data of as-prepared, 600 and 900 °C samples at 395 nm excitation

Sample	Gd^{3+} (at%)	I_1 (%)	τ_1 (ms)	I_2 (%)	τ_2 (ms)	τ_{av}[a] (ms)	χ^2[b]
ASP	0	81	0.42	19	0.65	0.46	0.99993
	5	98	0.49	2	1.36	0.51	0.99981
	10	98	0.48	2	1.25	0.49	0.99989
600 °C	0	96	0.48	4	0.95	0.50	0.99992
	5	96	0.50	4	1.0	0.52	0.99995
	10	99	0.48	2	1.29	0.48	0.99995
900 °C	0	100	0.47	0	—	0.47	0.99996
	5	97	0.43	3	0.89	0.44	0.99993
	10	94	0.44	6	0.57	0.44	0.99997

[a] $\tau_{av} = (I_1\tau_1 + I_2\tau_2)/(I_1 + I_2)$. [b] $\chi^2 = \sum_k \frac{w_k{}^2[X_k - F_k]^2}{n}\chi^2$ is goodness of fit, w_k is weighting factor for data points $\left(w_k = \frac{1}{\sqrt{F_k}}\right)$ and X_k and F_k be the calculated and measured life time data.

In the case of 0 at% Gd^{3+} co-doped $CaMoO_4$:Eu sample annealed at 900 °C under 395 nm excitation, we observed that the decay curve showed deviation from its bi-exponential (see Fig. S3(a)†) curve fit and fitted well with the mono-exponential function (Shown in Fig. S3(b)(ESI†)). Calculated lifetime values under 395 nm excitation of 0, 5 and 10 at% Gd^{3+} co-doped $CaMoO_4$:Eu for ASP, 600 and 900 °C using a mono-exponential curve fit are listed in Table S2 (ESI†). The average life time values for 5 and 10 at% Gd^{3+} doped 900 °C annealed samples show decrement as compared to ASP and 600 °C annealed samples. Wang and his co-workers[26] reported the decrease in lifetime values for Bi^{3+} co-doped $CaMoO_4$:Eu nanophosphors. Similar results were observed in cases of $Ca_2(Gd_{1-x}A_x)_8Si_6O_{26}$, A = Eu, Tb nanophosphor on annealing the samples above 800 °C.[49] It is worthwhile to mention the lifetime values reported in the literature for some other Eu^{3+} doped hosts. Since such a comparison will give an idea about the effect of Gd^{3+} doping and surface defects associated with the samples. Some of the reported lifetime of Eu^{3+} doped other hosts materials: Y_2O_3:Eu,[50] Gd_2O_3:Eu,[51] YVO_4:Eu,[52] $GdVO_4$:Eu,[42] and $LaPO_4$:Eu[53] are ~1.763, 1.56, 0.247, 0.583 and 3.56 ms, respectively.

The radiative rate constant is calculated from the reciprocal of lifetime ($K = 1/\tau_{av}$). Values of radiative rate constants using a bi-exponential curve fit under 395 nm excitation for 0, 5 and 10 at% Gd^{3+} co-doped $CaMoO_4$:Eu are 2.17×10^3, 1.96×10^3 and 2.04×10^3 s^{-1}, respectively for ASP samples; 2.0×10^3, 1.92×10^3 and 2.08×10^3 s^{-1}, respectively for 600 °C annealed samples; and 2.12×10^3, 2.27×10^3 and 2.27×10^3 s^{-1}, respectively for 900 °C annealed sample. Radiative rate constants for the mono-exponential curve fit for 0, 5 and 10 at% Gd^{3+} co-doped $CaMoO_4$:Eu under 395 nm excitation for ASP, 600 and 900 °C annealed samples are given in Table S3 (ESI†).

4.2.5 CIE study. The Commission Internationale de l'Eclairage (CIE) study have been performed on Gd^{3+} (0, 2, 5, 7 and 10 at%) co-doped $CaMoO_4$:Eu samples for ASP, 600 and 900 °C annealed samples. Typical CIE co-ordinates of 5 at% Gd^{3+} co-doped $CaMoO_4$:Eu for ASP, 600 and 900 °C are found to be (0.5334, 0.3711), (0.5331, 0.3708) and (0.6068, 0.3614), respectively. Detailed analysis of CIE co-ordinates of Gd^{3+}(0, 2, 5, 7 and 10 at%) co-doped $CaMoO_4$:Eu samples for ASP, 600 and 900 °C annealed are given in Table S4 (ESI†).

5. Conclusions

From PLE study, strong overlapping of Eu–O and Gd^{3+}/Mo–O charge transfer bands was observed. Absorption/excitation intensity increases with Gd^{3+} indicating energy transfer from Gd^{3+}/Mo–O to Eu^{3+}. Band gap decreases with annealing. In the photoluminescence study of Gd^{3+} co-doped $CaMoO_4$:Eu, the optimum PL intensity values are found at 2, 7 and 10 at% for ASP, 600 and 900 °C samples, respectively. Enhancement of luminescence was found with annealing due to the extent of the decrease of non-radiative rates arising from surface dangling bonds and –OH ions to the surface of the samples. The asymmetric ratios (A_{21}) of electric to magnetic dipole transitions are found to be in the range of ~12–16, which is relatively higher than those reported. The room temperature emission spectrum is dominated by the $^5D_0 \rightarrow {}^7F_2$ transition at 613 nm. Emission quantum yields up to 80% were obtained under excitation at 277 nm for ASP 10 at% Gd^{3+} co-doped $CaMoO_4$:Eu. From the photoluminescence decay studies on direct excitation at 395 nm and indirect excitation at 277 nm, energy transfer from Gd/Mo–O CT band to Eu^{3+} occurs. PL intensity variations have been studied in polar solvents; and found that these nanoparticles are dispersible and these dispersed particles can be incorporated in polyvinyl alcohol to make a film. The film shows the dark red emission after UV-radiation which can be useful in display devices. The CIE co-ordinates for 5 at% Gd^{3+} co-doped with $CaMoO_4$:Eu^{3+} for ASP, 600 and 900 °C were found to be (0.5334, 0.3711), (0.5331, 0.3708) and (0.6068, 0.3614), respectively. Through this study, we have demonstrated high quality luminescent material by incorporating Gd^{3+} ion, which is of great importance in improving the luminescence efficiency of the red phosphor at a much lower cost.

Acknowledgements

One of the authors (B. P. Singh) is thankful to Ministry of Human Resource and Development (MHRD) for providing financial support in the form of teaching assistantship.

References

1 V. M. Longo, L. S. Cavalcante, E. C. Paris, J. C. Sczancoski, P. S. Pizani, M. S. Li, J. Andres, E. Longo and J. A. Varela, *J. Phys. Chem. C*, 2011, **115**, 5207.
2 V. S. Marques, L. S. Cavalcante, J. C. Sczancoski, A. F. P. Alcantara, M. O. Orlandi, E. Moraes, E. Longo, J. A. Varela, M. S. Li and M. R. M. C. Santos, *Cryst. Growth Des.*, 2010, **10**, 4752.
3 V. M. Van der Ende, L. Arts and A. Meijerink, *Phys. Chem. Chem. Phys.*, 2009, **11**, 11081.
4 A. N. Annenkov, O. A. Buzanov, F. A. Danevich, A. S. Georgadze, S. K. Kim, H. J. Kimd, Y. D. Kim, V. V. Kobychev, V. N. Kornoukhov, M. Korzhik, J. I. Lee, O. Missevitchg, V. M. Mokina, S. S. Nagorny, A. S. Nikolaiko, D. V. Poda, R. B. Podviyanukb, D. J. Sedlak, O. G. Shkulkova, J. H. So, I. M. Solsky, V. I. Tretyakb and S. S. Yurchenkob, *Nucl. Instrum. Methods Phys. Res., Sect. A*, 2008, **584**, 334.
5 A. K. Parchur, R. S. Ningthoujam, S. B. Rai, G. S. Okram, R. A. Singh, M. Tyagi, S. C. Gadkari, R. Tewari and R. K. Vatsa, *Dalton Trans.*, 2011, **40**, 7595.
6 A. K. Parchur, A. I. Prasad, A. A. Ansari, S. B. Raia and R. S. Ningthoujam, *Dalton Trans.*, 2012, **41**, 11032.
7 G. S. R. Raju, E. Pavitra, Y. H. Ko and J. S. Yu, *J. Mater. Chem.*, 2012, **22**, 15562.
8 Y. Jin, J. Zhang, S. Lu, H. Zhao, X. Zhang and X. Wang, *J. Phys. Chem. C*, 2008, **112**, 5860.
9 J. Zhong, H. Liang, Q. Su, J. Zhou, Y. Huang, Z. Gao, Y. Tao and J. Wang, *Appl. Phys. B: Lasers Opt.*, 2010, **98**, 139.
10 E. Cavalli, P. Boutinaud, R. Mahiou, M. Bettinelli and P. Dorenbos, *Inorg. Chem.*, 2010, **49**, 4916.
11 S. Mahlik, M. Behrendt, M. Grinberg, E. Cavalli and M. Bettinelli, *J. Phys.: Condens. Matter*, 2013, **25**, 105502.
12 Y. Jin, J. Zhang, Z. Hao, X. Zhang and X. J. Wang, *J. Alloys Compd.*, 2011, **509**, L348.
13 J. H. Chung, S. Y. Lee, K. B. Shim, S. Y. Kweon, S. C. Ur and J. H. Ryu, *Appl. Phys. A: Mater. Sci. Process.*, 2012, **108**, 369.
14 W. Ren, G. Tian, L. Zhou, W. Yin, L. Yan, S. Jin, S. Li, Z. Gu and Y. Zhao, *Nanoscale*, 2012, **4**, 3754.
15 B. K. Gupta, V. Rathee, T. N. Narayanan, P. Thanikaivelan, A. Saha, Govind, S. P. Singh, V. Shankar, A. A. Marti and P. M. Ajayan, *Small*, 2011, **7**, 1767.
16 W. Yin, L. Zhou, Z. Gu, G. Tian, S. Jin, L. Yan, X. Liu, G. Xing, W. Ren, F. Liu, Z. Pane and Y. Zhao, *J. Mater. Chem.*, 2012, **22**, 6974.
17 Y. Park and T. Hyeon, *Adv. Mater.*, 2009, **21**, 4467.
18 R. Kumar, M. Nyk, T. Y. Ohulchanskyy, C. A. Flask and P. N. Prasad, *Adv. Funct. Mater.*, 2009, **19**, 853.
19 X. M. Zhang, X. B. Qiao and H. J. Seo, *Curr. Appl. Phys.*, 2011, **11**, 442.
20 X. M. Zhang and H. J. Seo, *Phys. B*, 2010, **405**, 2436.
21 N. Guo, Y. Jia, W. Lü, W. Lv, Q. Zhao, M. Jiao, B. Shao and H. You, *Dalton Trans.*, 2013, **42**, 5649.
22 C. K. Chang and T. M. Chen, *Appl. Phys. Lett.*, 2007, **91**, 081902.
23 C. H. Huang, T. M. Chen, W. R. Liu, Y. C. Chiu, Y. T. Yeh and S. M. Jang, *ACS Appl. Mater. Interfaces*, 2010, **2**, 259.
24 C. H. Huang, L. Y. Luo and T. M. Chen, *J. Electrochem. Soc.*, 2011, **158**, J341.
25 C. H. Huang, T. W. Kao and T. M. Chen, *ACS Appl. Mater. Interfaces*, 2010, **2**, 1395.

26 S. Yan, J. Zhang, X. Zhang, S. Lu, X. Ren, Z. Nie and X. Wang, *J. Phys. Chem. C*, 2007, **111**, 13256.
27 A. Xie, X. Yuan, S. Hai, J. Wang, F. Wang and L. Li, *J. Phys. D: Appl. Phys.*, 2009, **42**, 105107.
28 J. Liu, H. Lian and C. Shi, *Opt. Mater.*, 2007, **29**, 1591.
29 R. S. Ningthoujam, *Enhancement of luminescence by rare earth ions doping in semiconductor host*, ed. S. B. Rai and Y. Dwivedi, Nova Science Publishers Inc, USA, 2012, ch. 7, pp. 145–182.
30 W. R. Romanowski, S. Golab, G. D. Dzik and P. Solarz, *Appl. Phys. A: Mater. Sci. Process.*, 2002, **74**, 581.
31 Y. C. Li, Y. H. Chang, Y. S. Chang, Y. J. Lin and C. H. Laing, *J. Phys. Chem. C*, 2007, **111**, 10682.
32 N. K. Sahu, R. S. Ningthoujam and D. Bahadur, *J. Appl. Phys.*, 2012, **112**, 014306.
33 B. P. Singh, A. K. Parchur, R. S. Ningthoujam, A. A. Ansari, P. Singh and S. B. Rai, Influence of Gd^{3+} co-doping on Structural Property of $CaMoO_4$:Eu, *Dalton Trans.*, 2014, DOI: 10.1039/c3dt52786g.
34 D. L. Wood and J. Tauc, *Phys. Rev. B: Solid State*, 1972, **5**, 3144.
35 T. Thongtem, S. Kungwankunakorn, B. Kuntalue, A. Phuruangrat and S. Thongtem, *J. Alloys Compd.*, 2010, **506**, 475.
36 Z. Hou, R. Chai, M. Zhang, C. Zhang, P. Chong, Z. Xu, G. Li and J. Lin, *Langmuir*, 2009, **129**, 101.
37 F. Lei and B. Yan, *J. Solid State Chem.*, 2008, **181**, 855.
38 N. Yaiphaba, R. S. Ningthoujam, N. S. Singh, R. K. Vatsa, N. R. Singh, S. Dhara, N. L. Misra and R. Tewari, *J. Appl. Phys.*, 2010, **107**, 034301.
39 G. S. R. Raju, J. Y. Park, H. C. Jung, B. K. Moon, J. H. Jeong and J. H. Kim, *J. Electrochem. Soc.*, 2011, **158**(2), J20.
40 R. S. Ningthoujam, L. R. Singh, V. Sudarsan and S. D. Singh, *J. Alloys Compd.*, 2009, **484**, 782.
41 T. Igarashi, M. Ihara, T. Kusunoki, K. Ohno, T. Isobe and M. Senna, *Appl. Phys. Lett.*, 2000, **76**, 1549.
42 N. S. Singh, R. S. Ningthoujam, L. R. Devi, N. Yaiphaba, V. Sudarsan, S. D. Singh, R. K. Vatsa and R. Tewari, *J. Appl. Phys.*, 2008, **104**, 104307.
43 C. Shang, H. Jiang, X. Shang, M. Li and L. Zhao, *J. Phys. Chem. C*, 2011, **115**, 2630.
44 M. Thomas, P. P. Rao, M. Deepa, M. R. Chandran and P. Koshy, *J. Solid State Chem.*, 2009, **182**, 203.
45 J. Shi, Y. Hou, W. Chu, X. Shi, H. Gu, B. Wang and Z. Shun, *Inorg. Chem.*, 2013, **52**, 5013.
46 C. Reichardt and T. Welton, *Solvents and Solvent Effects in Organic Chemistry*, Wiley-VCH Publishers, 4th edn, 2011.
47 N. S. Singh, R. S. Ningthoujam, M. N. Luwang, S. D. Singh and R. K. Vatsa, *Chem. Phys. Lett.*, 2009, **480**, 237.
48 R. T. Wegh, H. Donker, K. D. Oskam and A. Meijerink, *Science*, 1999, **283**, 663.
49 G. S. R. Raju, H. C. Jung, J. Y. Park, B. K. Moon, R. Balakrishnaiah, J. H. Jeong and J. J. H. Kim, *Sens. Actuators, B*, 2010, **146**, 395.
50 G. Jia, M. Yang, Y. Song, H. You and H. Zhang, *Cryst. Growth Des.*, 2009, **9**, 301.
51 Y. Liu, P. yang, W. Wang, H. Dong and J. Lin, *CrystEngComm*, 2010, **12**, 3717.
52 M. N. Luwang, R. S. Ningthoujam, S. K. Srivastava and R. K. Vatsa, *J. Mater. Chem.*, 2011, **21**, 5326.
53 G. Phaomei, R. S. Ningthoujam, W. R. Singh, N. S. Singh, M. N. Luwang, R. Tewari and R. K. Vatsa, *Opt. Mater.*, 2010, **32**, 616.